

# 1-Hydroxy-2(1H)-pyridinone-Based Chelators with Potential Catechol O-Methyl Transferase Inhibition and Neurorescue Dual Action against Parkinson's Disease

Joseph C. J. Bergin <sup>1</sup>, Kean Kan Tan <sup>1</sup>, Anya K. Nelson <sup>1</sup>, Cristina-Andreea Amarandei <sup>2</sup>,  
Véronique Hubscher-Bruder <sup>2</sup>, Jérémy Brandel <sup>2</sup>, Varvara Voinarovska <sup>3</sup>, Annick Dejaegere <sup>3</sup>,  
Roland H. Stote <sup>3</sup> and David Tétard <sup>1,\*</sup>

<sup>1</sup> Department of Applied Sciences, Faculty of Health and Life Sciences, Northumbria University, Newcastle upon Tyne NE1 8ST, UK; joejbergin@gmail.com (J.C.J.B.); tankeankiat@hotmail.com (K.K.T.); anyanelson98@outlook.com (A.K.N.)

<sup>2</sup> Université de Strasbourg, CNRS, IPHC UMR 7178, F-67000 Strasbourg, France; amarandei@unistra.fr (C.-A.A.); veronique.hubscher@unistra.fr (V.H.-B.); jbrandel@unistra.fr (J.B.)

<sup>3</sup> Institut de Génétique et de Biologie Moléculaire et Cellulaire (IGBMC), Institut National de La Santé et de La Recherche Médicale (INSERM), U1258/Centre National de Recherche Scientifique (CNRS), UMR7104/Université de Strasbourg, 67404 Illkirch, France; varvara.voinarovska@helmholtz-muenchen.de (V.V.); annick@igbmc.fr (A.D.); rstote@igbmc.fr (R.H.S.)

\* Correspondence: david.tetard@northumbria.ac.uk

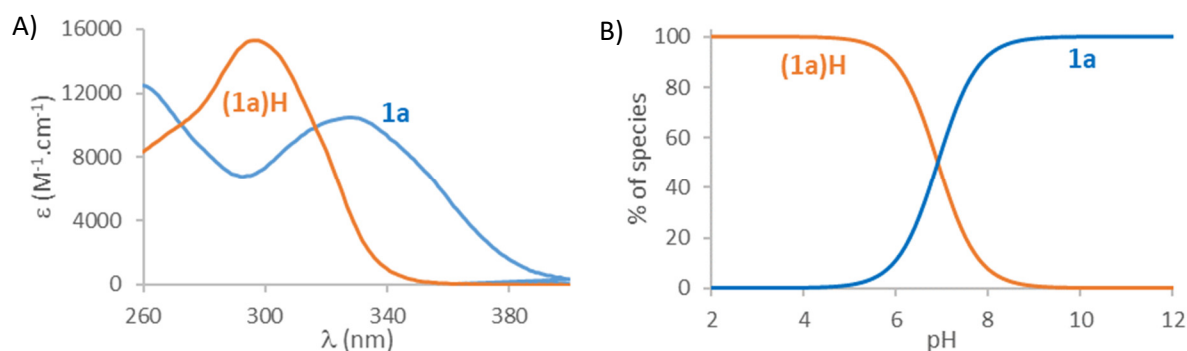


**Figure S1.** (A) Electronic spectra of the protonated species of ligand **1a** and (B) distribution curves of the protonated species of ligand **1a** ( $[\mathbf{1a}] = 1.00 \times 10^{-4}$  M). Solvent: MeOH/H<sub>2</sub>O (80/20 w/w), I = 0.1 M (NaClO<sub>4</sub>), T = 25.0 °C.

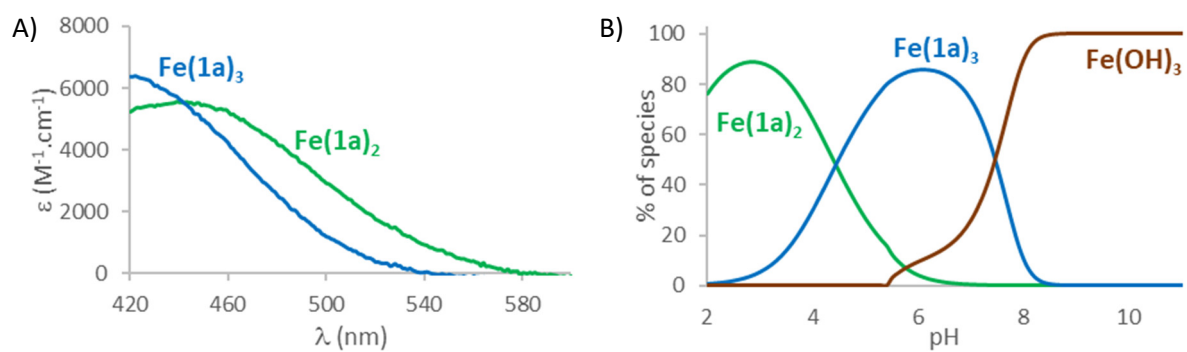


**Figure S2.** (A) Electronic spectra of  $\text{Fe}^{3+}$  complexes of **1a** and (B) distribution curves of  $\text{Fe}^{3+}$  complexes of **1a** relative to  $\text{Fe}^{3+}$  ( $[\mathbf{1a}] = 1.00 \times 10^{-4} \text{ M}$ ,  $[\text{Fe}^{3+}] = 3.20 \times 10^{-5} \text{ M}$ ). Solvent: MeOH/H<sub>2</sub>O (80/20 w/w),  $I = 0.1 \text{ M}$  ( $\text{NaClO}_4$ ),  $T = 25.0 \text{ }^\circ\text{C}$ .

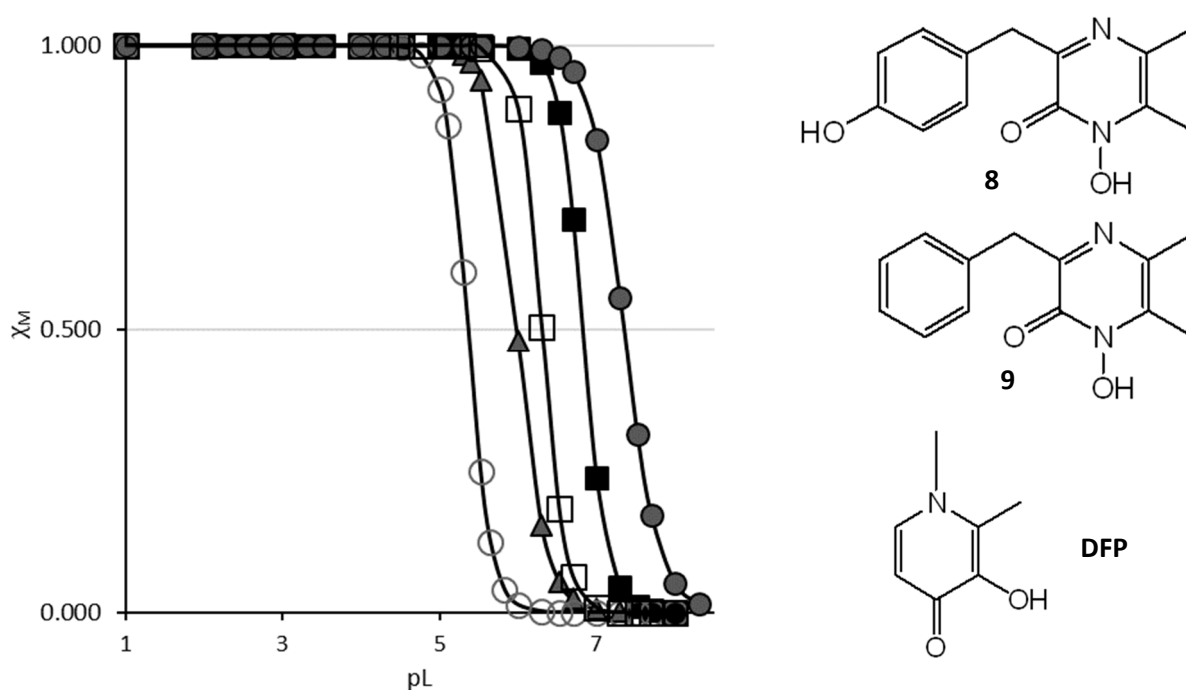


**Figure S3.** Sequestration diagrams towards  $\text{Fe}^{3+}$  at  $\text{pH} = 7.4$  of ligands (from left to right), **1a** (O), **6c** (▲), **1b** (□), DFP (■), **6d** (●) and  $[\text{Fe}^{3+}] = 10^{-9} \text{ M}$ ,  $T = 25.0 \text{ }^\circ\text{C}$ ,  $I = 0.1 \text{ M}$  ( $\text{NaClO}_4$ ).

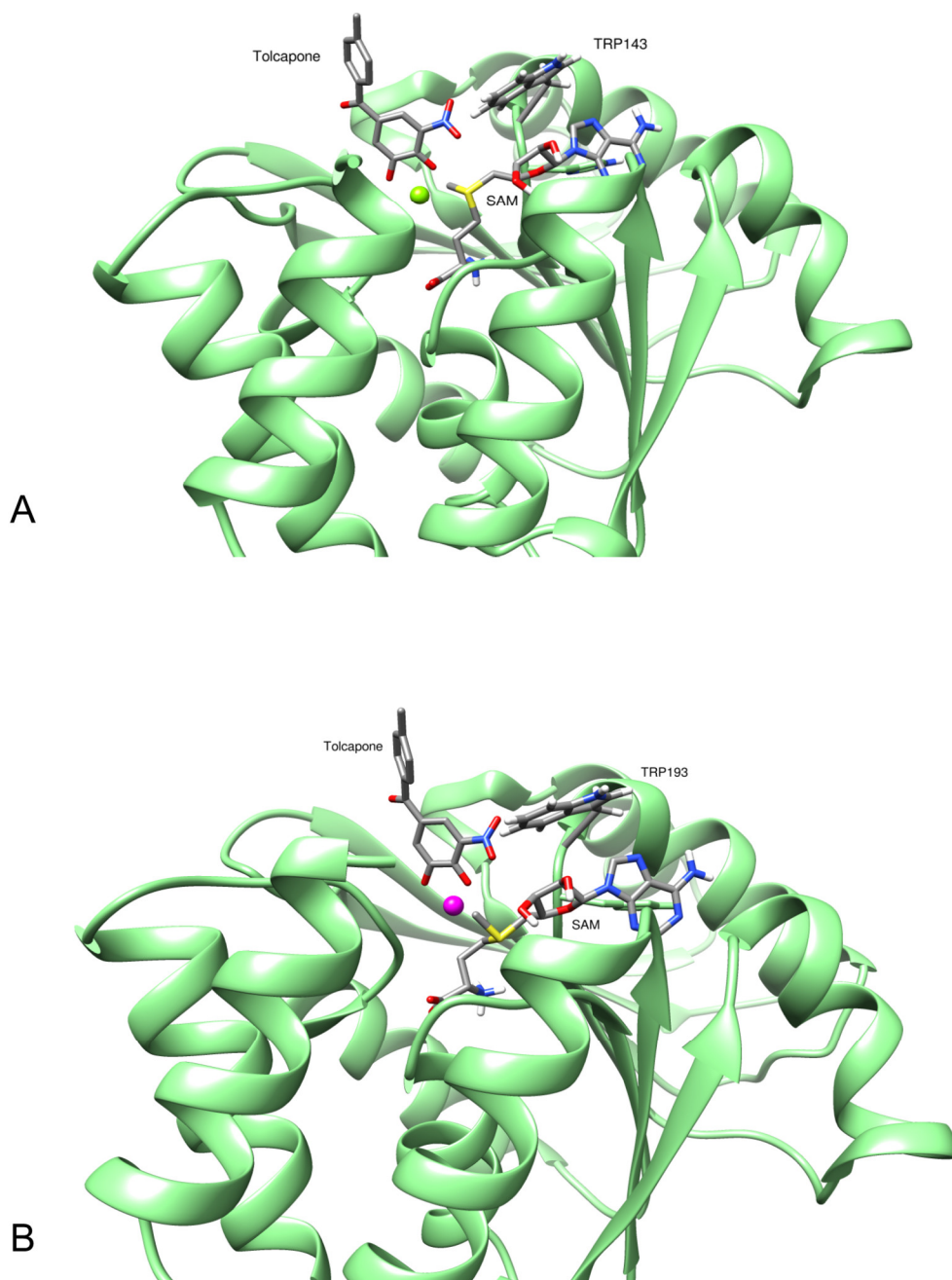


**Figure S4.** Starting conformations for the simulations of rat and human COMT in complex with Tolcapone, (A) rat COMT (PDBID 3S68), (B) human COMT (based on PDBID 5lsa)

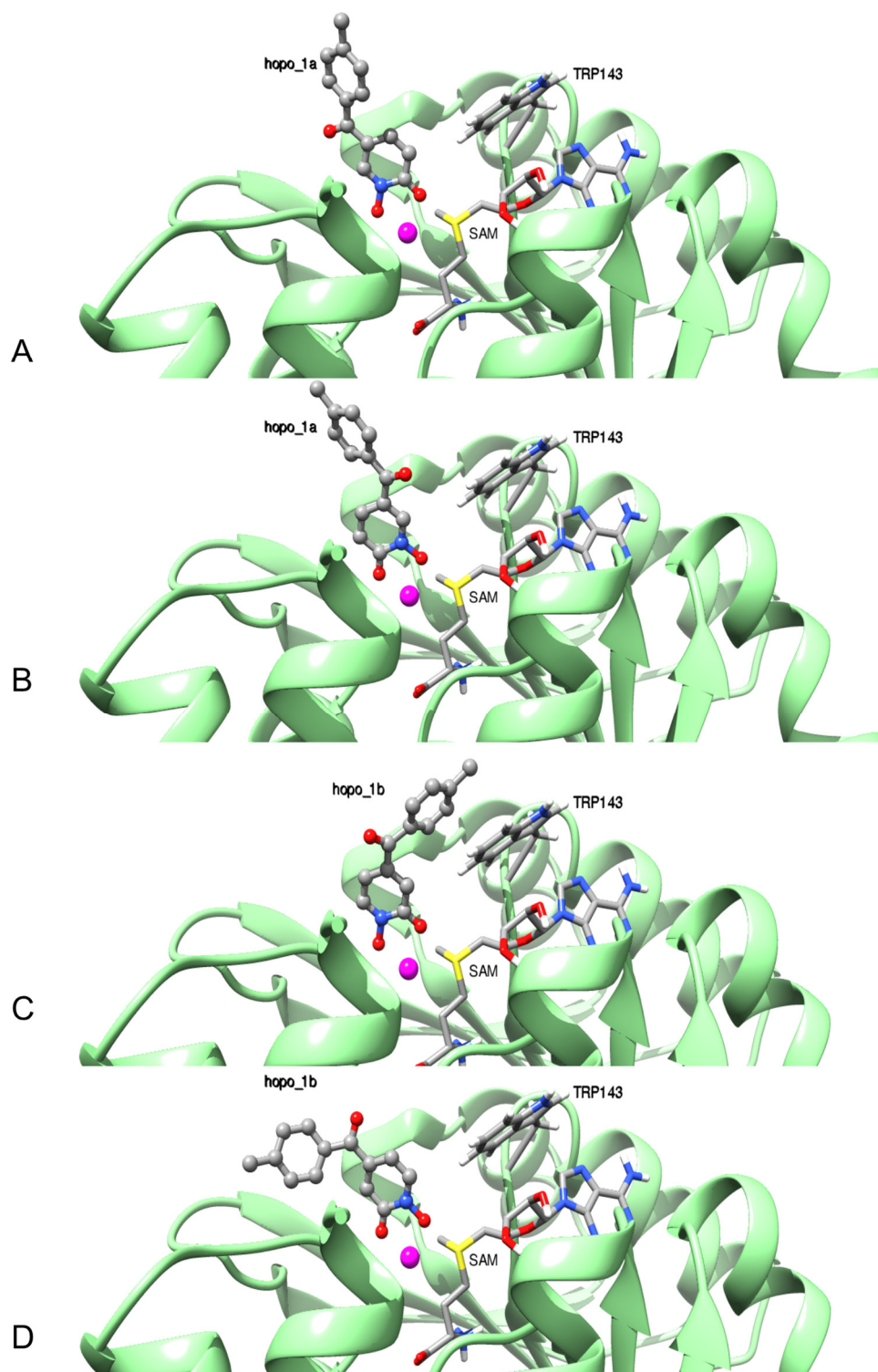


**Figure S5.** Starting conformations for the simulations of the rat COMT/HOPO complexes, based on PDBID 3S68. (A) **1a**, (B) **1a** with NO pointing toward SAM, (C) **1b**, D) **1b** with NO pointing towards SAM

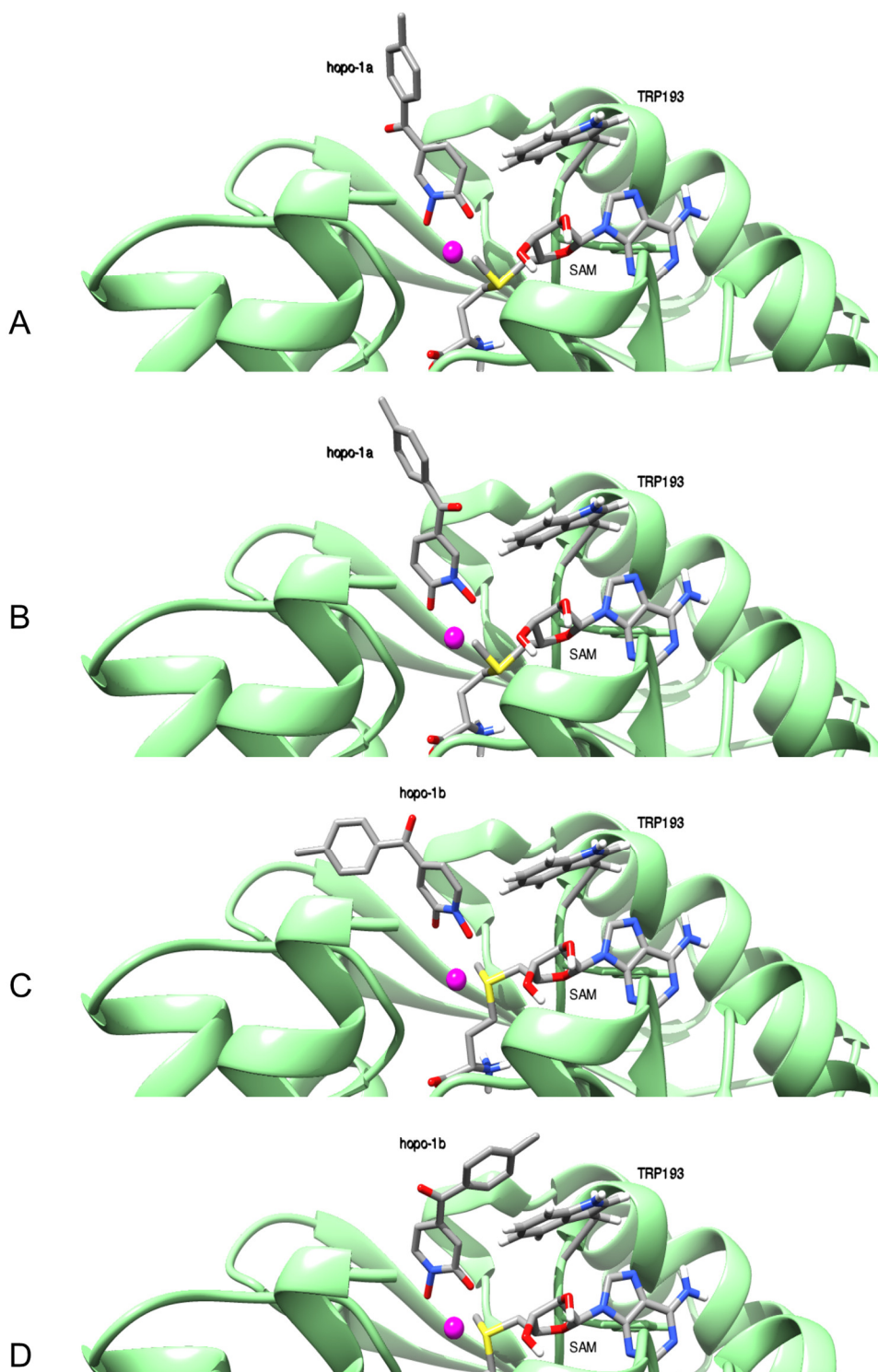


**Figure S6.** Starting conformations for the simulations of the human COMT/HOPO complexes, based on PDBID 3S68. (A) **1a**, (B) **1a** with NO pointing toward SAM, (C) **1b**, (D) **1b** with NO pointing towards SAM

RMSD in 3s68 COMT backbone

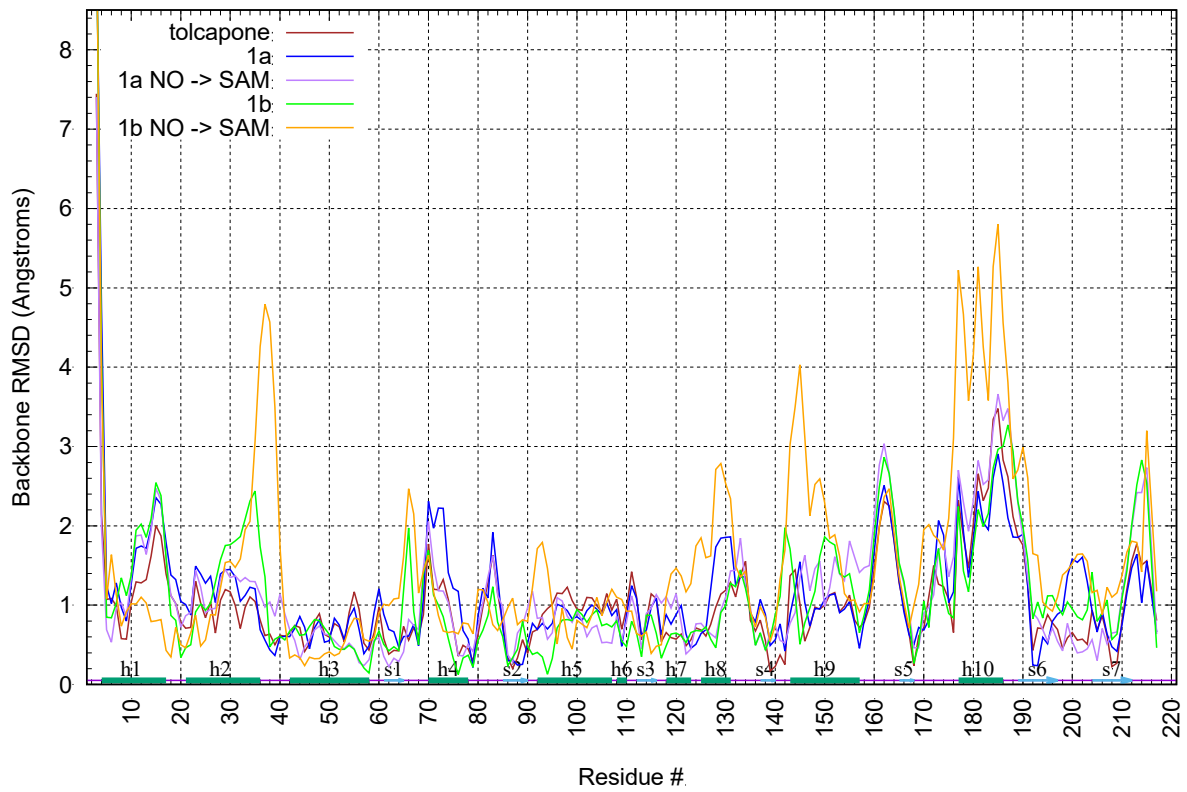


**Figure S7.** Backbone RMSD by-residue for average structures of the different rat COMT complexes calculated at the end of the simulation (averaged over 10ns)

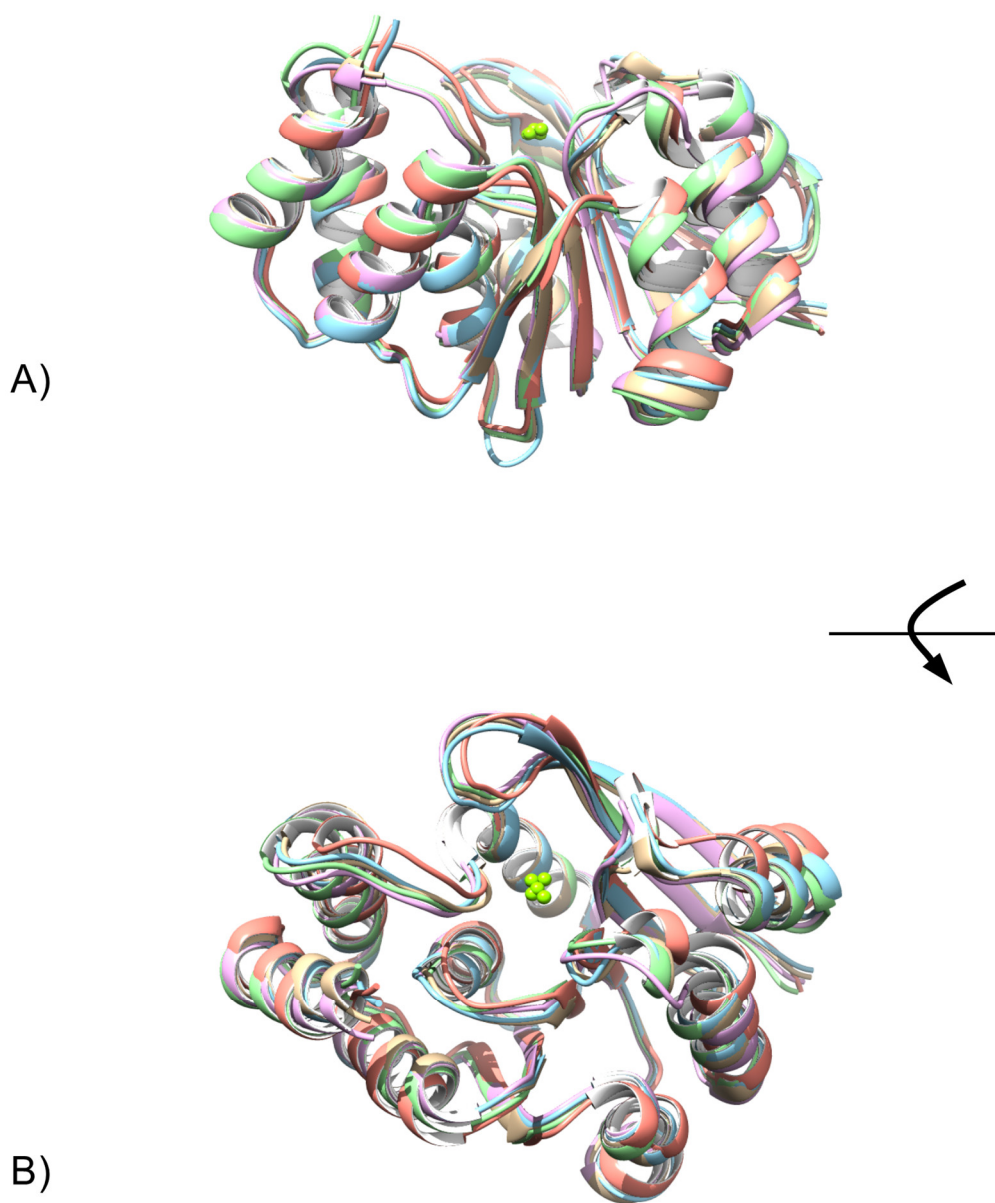


**Figure S8.** Superposition of average structures from the end of the MD simulations of the complexes of rat COMT, (A) a side view and (B) top-down view obtained by rotating 90° to look down at the ligand binding site with the Mg<sup>2+</sup> ion shown as a green sphere; colour legend, in complex with tolcapone in brown, with hopo-1a in blue (see Fig. 6a) , with hopo-1a\_NO->SAM in magenta (see Fig. 6b), with hopo-1b in green (see Fig. 6c), with hopo-1b\_NO->SAM in orange (see Fig. 6d)

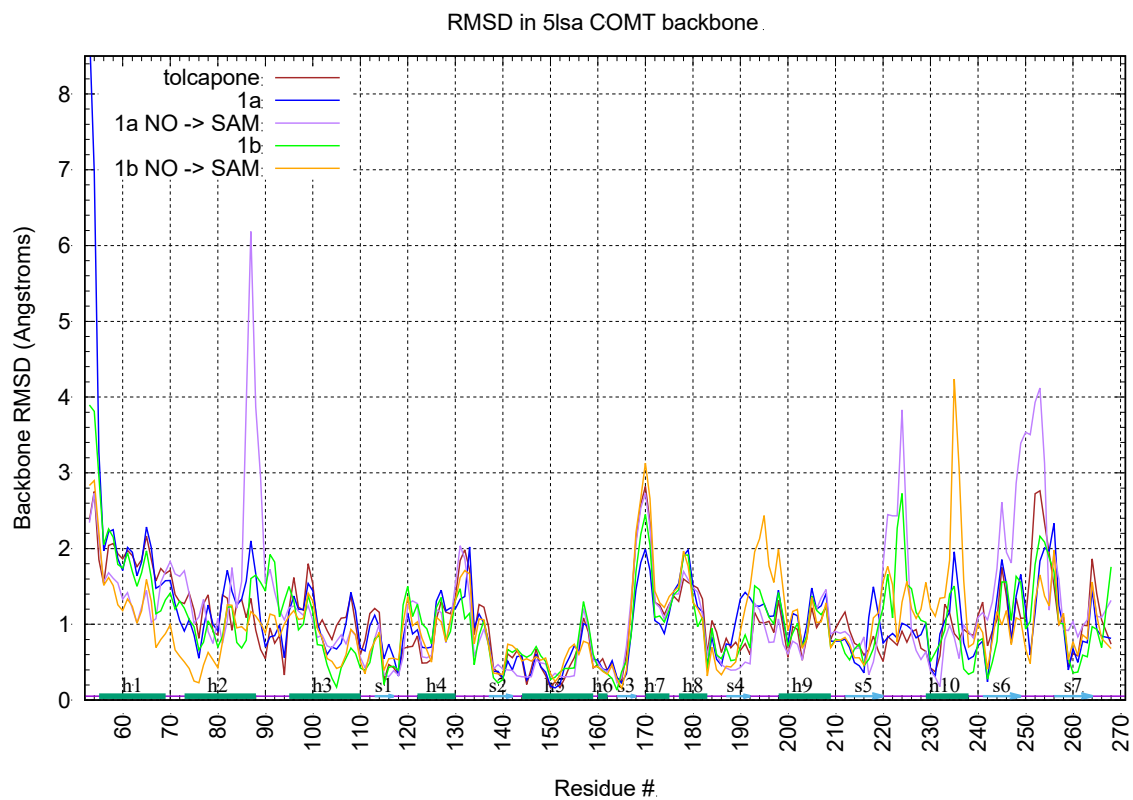


**Figure S9.** Backbone RMSD by-residue for average structures of the different human COMT complexes calculated at the end of the simulation (averaged over 10ns)

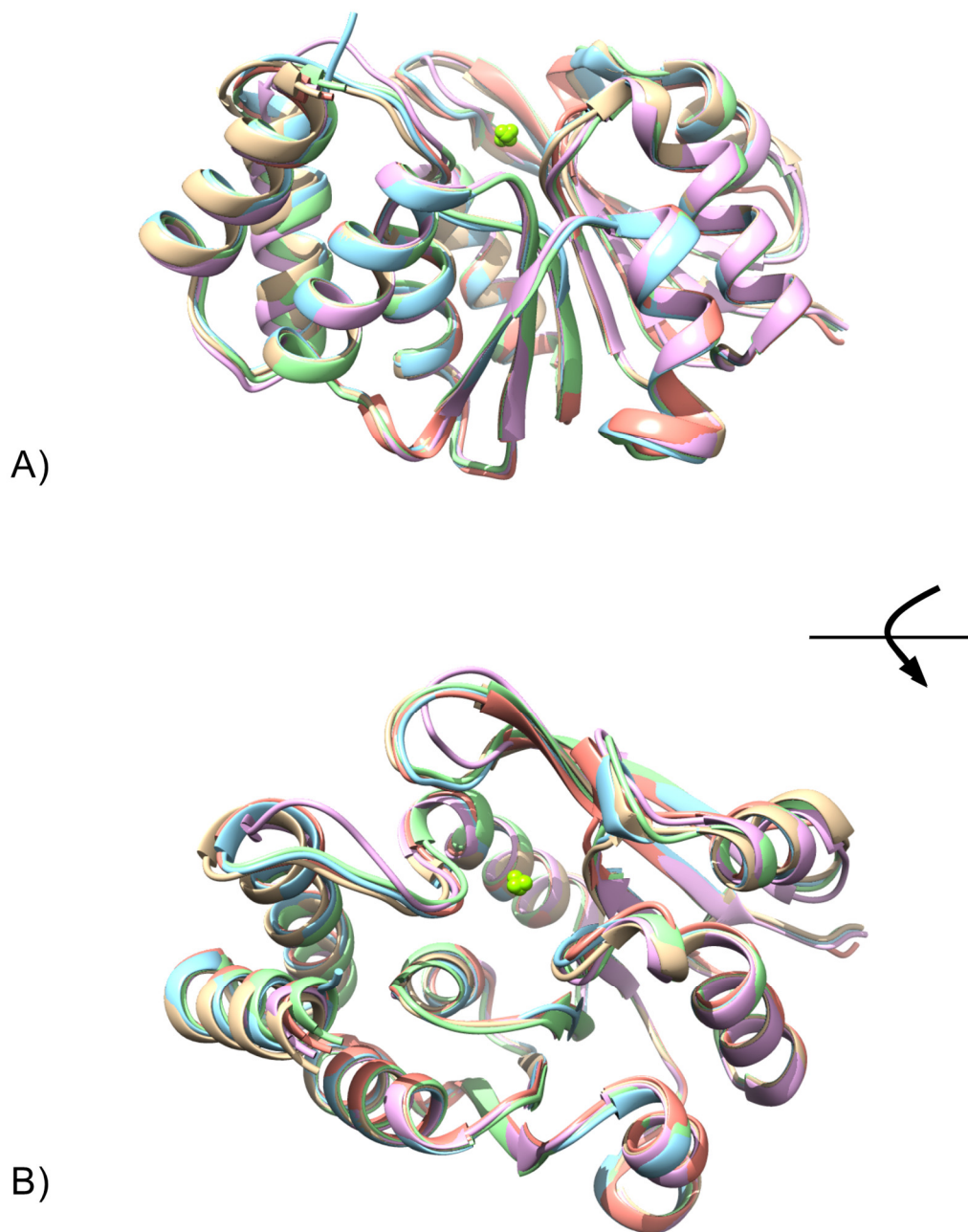


**Figure S10.** Superposition of average structures from the end of the MD simulations of the complexes of human COMT, (A) a side view and (B) top-down view obtained by rotating 90° to look down at the ligand binding site with the Mg<sup>2+</sup> ion shown as a green sphere; colour legend, with complex with tolcapone in brown, with hopo-1a in blue (see Fig. 6a) , with hopo-1a\_NO->SAM in magenta (see Fig. 6b), with hopo-1b in green (see Fig. 6c), with hopo-1b\_NO->SAM in orange (see Fig. 6d)

**Table S1.** Binding Free energy scores with absolute scores with standard deviations and differences between doubly protonated tolcapone score and the scores of the other compounds and orientations

Species	Ligand Orientation	$\Delta G_{\text{binding}}$ (kcal/mol)	$\Delta G_{\text{binding}}$ (Tol) - $\Delta G_{\text{binding}}$ (Compound)
Rat	Tolcapone doubly deprotonated (Fig 5a)	-30.9 ( $\pm 9.6$ )	0.0 ( $\pm 9.6$ )
Rat	Tolcapone singly deprotonated (Fig. 5b)	-13.0 ( $\pm 5.4$ )	17.9 ( $\pm 5.4$ )
Rat	HOPO-1a =O $\rightarrow$ SAM (Fig 6a)	+4.7 ( $\pm 5.9$ )	35.6 ( $\pm 5.9$ )
Rat	HOPO-1a N-O $\rightarrow$ SAM (Fig 6b)	-28.8 ( $\pm 5.1$ )	2.1 ( $\pm 5.1$ )
Rat	HOPO-1b N-O $\rightarrow$ SAM (Fig 6c)	-20.4 ( $\pm 5.7$ )	10.5 ( $\pm 5.7$ )
Rat	HOPO-1b =O $\rightarrow$ SAM (Fig 6d)	-27.6 ( $\pm 3.9$ )	3.3 ( $\pm 3.9$ )
Human	Tolcapone doubly deprotonated (Fig 1a)	-23.6 ( $\pm 5.4$ )	0.0 ( $\pm 5.4$ )
Human	Tolcapone singly deprotonated, (Fig 1b)	-17.8 ( $\pm 6.8$ )	5.8 ( $\pm 6.8$ )
Human	HOPO-1a =O $\rightarrow$ SAM (Fig 6a)	+7.8 ( $\pm 5.1$ )	31.4 ( $\pm 5.1$ )
Human	HOPO-1a N-O $\rightarrow$ SAM (Fig 6b)	-28.3 ( $\pm 5.3$ )	-4.7 ( $\pm 5.3$ )
Human	HOPO-1b N-O $\rightarrow$ SAM (Fig 6c)	-0.5 ( $\pm 4.9$ )	23.1 ( $\pm 4.9$ )
Human	HOPO-1b =O $\rightarrow$ SAM (Fig 6d)	-7.1 ( $\pm 4.7$ )	16.5 ( $\pm 4.7$ )